J. Phys. Chem. A **2009,** *113,* 931–937

Flexibility of the Saturated Five-Membered Ring in 2,5-Pyrrolidinedione (Succinimide): Electron Diffraction and Quantum-Chemical Studies with Use of Vibrational Spectroscopy Data

Natalja Vogt,*,[†] Leonid S. Khaikin,[†,‡] Olga E. Grikina,[†,‡] Nikolai M. Karasev,[‡] Jürgen Vogt,[†] and Lev V. Vilkov[‡]

Chemieinformationssysteme, Universität Ulm, 89069 Ulm, Germany, and Department of Chemistry, Moscow State University, Moscow 119992, Russia

Received: October 8, 2008

The flexibility of succinimide molecule has been studied for the first time by quantum-chemical (at the MP2 level with up to the 6−311G(3df,2p) basis sets) and gas-phase electron diffraction (GED) methods using vibrational spectroscopy data from literature. The analysis of vibrational spectra, performed for the molecular model of C_{2v} symmetry (predicted by high-level ab initio calculations) using the scaling procedure, has shown that the two out-of-plane ring motions, that is, ring-bending and ring-twisting, are practically pure modes of different symmetry types and can be considered separately. The one-dimensional potential curves for the ring-bending and ring-twisting vibrations calculated at the MP2(full)/6−311G(3df,2p) level could be approximated by harmonic and anharmonic functions, respectively. The diverged energy levels for the ring-twisting vibration and the constant transition frequencies for the bending motion, obtained by the solution of the direct one-dimensional problem for the nonrigid model, demonstrate this statement. In the GED analysis, the succinimide molecule with a large-amplitude ring-twisting motion was described by a dynamic model with the distribution of pseudoconformers according to the calculated potential function taking into account structural relaxation effects from the MP2(full)/6−311G(3df,2p) calculations. This model greatly improved the fit of the GED intensities (R factor decreased from 4.6% for static model to 2.8%). The equilibrium molecular parameters r_e determined in the dynamic approximation are very close to the corresponding values from the ab initio calculations. At the same time, the parameters of the $-CH_2-CH_2-$ fragment involved in the ring-twisting motion deviate considerably from those obtained for the static model (C−C bond length by 0.027 Å, =C−C−H, C−C−H, and H−C−C−N angles by up to 7°). The flexibility influence on the C−C bond length is several times larger than the calculated vibrational correction ($r_e - r_a$) as well as the experimental uncertainty.

1. Introduction

The flexibility of cyclic molecules is a very difficult topic for experimental as well as theoretical studies because low-energy conformational transformations and large-amplitude vibrational motions may need to be considered. The studies of relatively simple molecules with small rings (up to five-membered) are practically important to understand such phenomena in complicated systems, such as bio- and bioactive molecules. Depending on the ratio of substitution, conjugation, and other effects, the equilibrium conformations of these molecules can have various forms that are difficult to predict. So, the nonsubstituted cyclopentane was found to have pseudorotating nonplanar conformation,[1] whereas the succinic anhydride ring was determined to be essentially planar with the averaged torsional angle $\angle_a$(C−O−C−C) of 4.1(20)°.[2] To be less strained, the bond configurations at both C_{sp2} atoms of the carbonyl groups need enlarging of the adjusted ring angles in the succinic anhydride in comparison to those at the C_{sp3} atoms in the cyclopentane and thus lead to a planar ring conformation. Because of a lone electron pair, the N atom forms a nonplanar moiety in the molecule. However, in amides (see, e.g., formamide[3]), including peptides and proteins, the O=C−N< fragment should be planar because of the conjugation effect.

Five-membered ring conformations can be classified using two factors which control conformation: the ring angle strain and the potential energy barriers to torsional motion about ring bonds.[4] The increase of the ring angle strain is coupled with a reduction of the barriers to torsional motions about the bond involved. Both changes tend to favor the planar ring over the puckered one.

To answer the question about a conformation of the five-membered ring, the parameters of potential energy surface should be determined or estimated. Numerous theoretical models (various two-dimensional and effective one-dimensional potential functions) have been proposed in the literature (see, e.g., review papers[4−6] and references therein) to describe the individual five-membered rings (saturated, nonsaturated, with only carbon or heteroatoms, with different substituents at ring atoms, etc.). However, the flexibility of the saturated five-membered ring consisting of imide fragment (succinimide and its derivatives) has not been considered[4−6] and has not been studied yet experimentally.[7−10]

Being widespread in the chemistry of heterocycles and in biochemistry (e.g., succinimide as agent in ring-opening reactions,[11] *N*-hydroxysuccinimide as agent in activating the function of carboxy groups in peptide syntheses,[12] *N*-bromosuccinimide

---

* To whom correspondence should be addressed.

[†] Universität Ulm.

[‡] Moscow State University.

10.1021/jp8089177 CCC: $40.75

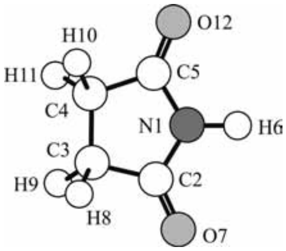

Figure 1. Molecular model of succinimide with atom numbering.

as mild bromination agent, etc.), such systems are of big interest. In the present work, the analysis of gas-phase electron diffraction (GED) intensities using vibrational spectroscopy data and results of ab initio calculations has been carried out to answer the questions of how flexible the succinimide molecule (Figure 1) is and which model is appropriate to describe its dynamics.

2. GED Experiment

The succinimide sample was purchased from Merck Co (purity > 99%) and was used without further purification. The GED experiment was carried out at the Moscow State University on the EG-100 M apparatus using the new r^3 sector from brass produced with high precision in the workshop of the University of Ulm. In comparison to the old handmade sector, which was used many years in the Moscow GED laboratory, the new unit, which was milled more exactly, has a significantly better sector function yielding a smoother background. This unit was successfully applied for the first time in ref 13. The experimental conditions were the following: accelerating voltage of ca. 57 kV, electron beam current of 2.2 μA, and vacuum of $2 \cdot 10^{-5}$ mm Hg. The necessary sample pressure of a few Torr was reached at 119(3) °C. The diffraction patterns were recorded on photo films (MACO EM-FILM EMS) at the long (LD) and short (SD) nozzle-to-film distances of 362.16 and 193.82 mm, respectively. The patterns of CCl_4 were recorded to calibrate the wavelength of the electron beam. The structural parameters of the CCl_4 molecule were taken from ref 14. The differences between wavelengths of electrons at the beginning and at the end of each of two experiments (LD and SD) were less than 0.02%. The diffraction patterns were scanned at the University of Ulm using the EPSON PERFECTION V750 PRO commercial scanner in the 16-bit/300dpi scanning mode. The calibration of the scanner was carried out using a gray scale for Kodak ektachrome films. Data of scanning were transformed into intensity curves $I(s)$ using the program UNEX which follows the method described in ref 15.

The experimental intensities $I(s)$ were averaged in the ranges of $s = 3.0-18.5$ Å^{-1} (LD) and $s = 7.0-33.75$ Å^{-1} (SD) in steps of 0.125 and 0.25 Å^{-1}, respectively. The averaged $I(s)$ curves are presented in Table 1S and Figure 1S of the Supporting Information.

3. Ab Initio Calculations

The quantum-chemical calculations have been carried out to (1) determine the molecular symmetry, structural differences between similar molecular parameters, and potential functions for intramolecular motions and (2) estimate force fields which are necessary for the calculation of vibrational corrections to internuclear distances and root-mean-square (rms) vibrational amplitudes and for the analysis of vibrational spectra. They were performed at the MP2(full) level of theory using 6−311G(d,p), 6−311G(2df,p), cc-pVTZ, and 6−311G(3df,2p) basis sets by means of the GAUSSIAN03 program package.[16]

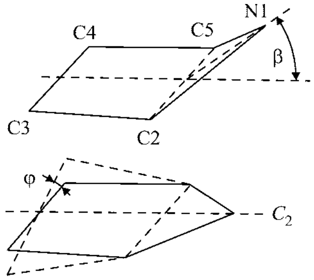

Figure 2. Definitions of the ring-bending $x = r \cdot \beta$ and ring-twisting φ coordinates.

The minimum of the potential surface determined by the calculation with the relatively simple 6−311G(d,p) basis set corresponds to the C_2 structure with nonplanar ring lying only 18 cal/mol lower than the transition state of C_{2v} symmetry and having geometrical parameters insufficiently different from those for the C_{2v} structure. The conformation optimizations with the extended (6–311G(2df,p), cc-pVTZ, and 6−311G(3df,2p) basis sets converged to the C_{2v} structure with the planar ring. The results are presented in Table 2S of the Supporting Information. The absence of imaginary frequencies confirmed that the determined conformations correspond to the minima on the potential surfaces.

In general, the out-of-plane vibrations of five-membered rings have two degrees of freedom and should be presented as the ring-twisting and ring-bending motions. For succinimide, the ring-twisting and ring-bending correspond to the oscillations of the C_{sp3} atoms and the out-of-plane deviation of the flap N atom, respectively. The corresponding coordinates, φ and β angles, describing these motions are shown in Figure 2. The cross sections of the potential energy surface along the φ and β coordinates were calculated in the MP2(full)/6−311G(3df,2p) approximation. The one-dimensional ring-twisting and ring-bending potential functions will be considered below in detail (see section 5).

Quadratic and cubic force constants and fundamental frequencies were calculated at the MP2(full)/6−311G(3df,2p) level. Very time consuming numerical calculations of anharmonic force constants were carried out at the University of Ulm (Group of Chemical Information Systems) by means of a new version of Gaussian program G03-Rev.E.01 which allowed parallelization of such calculations.

4. Vibrational Analysis

Since gas-phase and matrix-isolated vibrational spectra of the succinimide molecule are absent, the spectra of the parent[17−19] and N-d_1[17,20] isotopic species in different solvents and in solid state were considered instead. The normal coordinate analysis was carried out by fitting the calculated frequencies to the experimental ones using Pulay's method[21,22] of scaling quantum chemical force field by means of the program written by Krasnoshchekov.[23] The nonredundant set of local symmetry internal coordinates, the determined scale factors for the MP2(full)/6−311G(3df,2p) force constants, and our assignment of the experimental spectra and the scaled force constants in comparison with literature data[17,24] are presented in Tables 3S, 4S, and 5S of the Supporting Information, respectively.

According to the solution of the vibrational problem, the ring-twisting and ring-bending are practically pure modes of different symmetry types, A_2 and B_1, with potential energy distribution (PED) of 97 and 96%, respectively, and consequently, they are independent. These motions belong to the lowest-energy vibra-

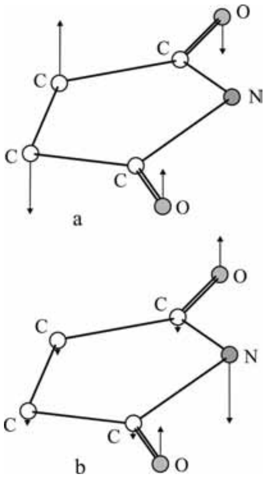

Figure 3. Ring-twisting (a) and ring-bending (b) vibrational modes.

tions in the molecule. Moreover, for the ring-twisting motion, the vibrational frequency of 54 cm^{-1} and quadratic force constant of 0.04 mdyn·Å are considerably lower in comparison to those for the ring-bending motion (133 cm^{-1} and 0.18 mdyn·Å, respectively). The ring-twisting motion is characterized by the most intensive vibrations of CH_2-groups and the relatively weak vibrations of O atoms (see Figure 3). In the ring-bending motion, the N−H fragment mainly participates.

Spectroscopic calculations were performed using the ANCO/SCAL/PERT[23] and SHRINK-07 (updated 2007 version)[25,26] program packages.

5. One-Dimensional Potential Functions of the Ring-Twisting and Ring-Bending Motions

According to results of the vibrational spectra analysis (see previous section), the ring-twisting and ring-bending motions are independent and can be described separately.

The potential energy curve of the ring-bending motion as a function of the ring-bending angle β was calculated in the interval 2.5° $\leq \beta \leq$ 32.5° with steps of 5° at the MP2(full)/6−311G(3df,2p) level with optimization of remaining geometrical parameters. Taking into account the symmetry of the potential function because of the symmetry of the molecule and the position of the minima determined in the full geometry optimization, this curve can be presented by 15 points. Further, the ring-bending coordinate β was transformed into the inversion coordinate $x = r{\cdot}\beta$,[27,28] where r is the distance from the N atom to the bending axis C2...C5 (see Figure 2) and β is in radians. The obtained potential curve $V(x)$ (in cm^{-1}) could be approximated by a quadratic function with a standard deviation less than 5 cm^{-1} as well as by an anharmonic function with the first V_2 and V_4 even coefficients of a power series (see Table 1) and a standard deviation of ca. 1 cm^{-1}. The $V(x)$ energy profile from the ab initio calculations and its approximations by the quadratic and quadratic-quartic functions are so close to each other that they look like one line (Figure 2S of Supporting Information).

The kinetic energy function $g_{44}(x)$[29] was calculated using the geometrical parameters of the molecule from MP2(full)/6−311G(3df,2p) calculations for the corresponding x points. The obtained $g_{44}(x)$ function could be approximated with a high accuracy by the first four even coefficients of the truncated power series presented in Table 1. The energy spectrum was estimated by the direct solution of the one-dimensional problem for the nonrigid model according to ref 30. The calculated transition frequencies are listed in Table 1. Being practically constant, these frequencies together with the harmonic potential curve shape testify to a harmonic character of the ring-bending motion.

The potential function of the ring-twisting motion, $V(\varphi)$, was determined for the ring-twisting angle φ in the interval from 0° to 30° with steps of 2.5° at MP2(full)/6−311G(3df,2p) level with optimization of the remaining geometrical parameters of the molecule. The considerable variations of nonbonded distances between heavy atoms (up to 0.1 Å) as functions of φ are presented in Figure 3S of the Supporting Information. The obtained deviations in the bond lengths during the twisting vibration were relatively small (up to 0.002 Å, except for the C−N bond with the variation of 0.007 Å). The relaxation effects will be further taken into account for the description of the dynamic molecular model in the GED analysis.

Considering the position of minima, determined in full geometry optimization, and the symmetry of the potential function, the $V(\varphi)$ curve can be presented by 25 points. The determined curve (Figure 4S of Supporting Information) could not be successfully approximated by a quadratic function (one standard deviation was more than 100 cm^{-1}). This fact reflects a high anharmonicity of the ring-twisting motion. Therefore, in the following, this motion was considered as a torsion in the limited interval of the coordinate φ with the potential energy function approximated by the truncated Fourier series

$$V(\varphi) = V_0 + 0.5 \sum_{k=3,5} V_k(1 - \cos k\varphi)$$

in which the sinus terms were omitted because of the symmetry of the molecule. The coefficients of the series, determined by fitting the Fourier functional to $V(\varphi)$ from ab initio calculations, are listed in Table 2. The kinetic energy function was described by the functional

$$F(\varphi) = \sum_{k=0}^{12} F_k \cos k\varphi$$

The coefficients F_k calculated using the geometrical parameters of the molecule from the MP2(full)/6−311G(3df,2p) calculations are given in Table 2. The energy levels and transition frequencies were obtained by the solution of the direct one-dimensional problem for the nonrigid model.[30] As can be seen from Table 2, the transition frequencies diverge very strongly. Thus, the anharmonic potential curve shape and diverged energy levels point to anharmonic character of the ring-twisting motion in succinimide.

In summary, it can be concluded that the one-dimensional potential functions of the ring-bending and ring-twisting motions are essentially different, being harmonic and anharmonic, respectively. The shape of the anharmonic potential function points to the large-amplitude motion, that is, the flexibility of the ring.

6. Analysis of the GED Data Supplemented by Results of ab Initio and Spectroscopic Calculations

The analysis of the GED data was performed in terms of equilibrium r_e structure which was derived from the conventional thermal-average $r_{ij,a}$ parameters. These transformations as well as the calculations of the rms amplitudes were carried out taking into account nonlinear kinematic effects at the level of the first-order perturbation theory.[26,31] The harmonic ($\delta_{ij,\mathrm{h1}}$, including also centrifugal distortions due to vibrations[32]) and anharmonic ($\delta_{ij,\mathrm{anh1}}$[31]) corrections were calculated using scaled quadratic and cubic force fields from the MP2(full)/6−311G(3df,2p) calculations. Corrections for the centrifugal distortion effects due to

TABLE 1: Parameters of Kinetic $g_{44}(x)$ and Potential $V(x)$ Energy Functions for the Ring-Bending Vibration Calculated at the MP2(Full)/6-311G(3df,2p) Level and Approximated by a Power Series[a]

power k	$g_{44}(x) \times 10^2$, amu^{-1} Å^{-2}	$V(x)$, cm^{-1} harmonic	$V(x)$, cm^{-1} anharmonic	level	E, cm^{-1}	transition	ν, cm^{-1}
0	7.471042	0.0	0.0	0	99.0	0 → 1	197.6
2	2.334925	7710.673	7749.071	1	296.6	1 → 2	197.6
4	−4.078543		−692.356	2	494.2	2 → 3	197.6
6	5.131603			3	691.8	3 → 4	197.6
				4	889.4	4 → 5	197.6
σ[b]	2.77×10^{-2}	4.871	0.768	5	1086.9	5 → 6	197.5

[a] Energy levels and frequencies of transitions calculated with V_2 and V_4 terms of the potential function. Coordinate x is in Å (see text). [b] σ is the estimated standard error of the fitting.

TABLE 2: Parameters of Kinetic $F(\varphi)$ and Potential $V(\varphi)$ Functions,[a] **Energy Levels, and Transition Frequencies of the Ring-Twisting Vibration**

k	$F_k \times 10^3$, cm^{-1}	V_k, cm^{-1}	level	E, cm^{-1}	transition	ν, cm^{-1}
0	816.585	−0.05	0	46.3	0 → 1	103.4
1	15.518		1	149.7	1 → 2	120.9
2	2.702		2	270.6	2 → 3	132.6
3	−8.108	12871.3	3	403.2	3 → 4	142.0
4	1.015		4	545.2	4 → 5	149.6
5	−3.107	−4346.3	5	694.8	5 → 6	156.2
6	0.688		6	851.0	6 → 7	162.0
7	−1.575		7	1013.0	7 →8	167.0
8	0.560		8	1180.0	8 → 9	171.6
9	−0.947		9	1351.6	9 → 10	175.7
10	0.489		10	1527.3		
11	−0.649					
12	0.444					
σ[b]	1.86×10^{-5}	2.33				

[a] Calculated at the MP2(full)/6-311G(3df,2p) level and approximated by the series. See text. [b] σ is estimated standard error of the fitting.

TABLE 3: Vibrational Corrections to the Experimental Internuclear Distances ($r_e - r_a$) and rms Vibrational Amplitudes (u) Calculated Using the Scaled MP2(Full)/6-311G(3df,2p) Force Field with their Deviations from the Experimental Values for the Dynamic Molecular Model[a]

distance[b]	r_e	$r_e - r_a^{\mathrm{fr}}$	$u_{\mathrm{h0}}^{\mathrm{fr}}$	$u_{\mathrm{h1}}^{\mathrm{fr}}$	$u_{\mathrm{exp}}^{\mathrm{fr}} - u_{\mathrm{h1}}^{\mathrm{fr}}$
N−H	1.007(18)	−0.0149	0.0724	0.0724	0.0[c]
C−H	1.086(7)	−0.0160	0.0781	0.0781	0.0[c]
C=O	1.202(1)	−0.0037	0.0385	0.0385	−0.0005(10)
N−C	1.376(2)	−0.0113	0.0464	0.0465	0.0006(13)[d]
=C−C	1.520(4)	−0.0076	0.0524	0.0524	0.0006(13)[d]
C−C	1.526(5)	−0.0072	0.0520	0.0521	0.0006(13)[d]
N...O	2.299(3)	−0.0111	0.0548	0.0549	0.0016(14)[e]
N...C	2.318(5)	−0.0137	0.0556	0.0559	0.0016(14)[e]
=C...C=	2.339(3)	−0.0093	0.0529	0.0535	0.0016(14)[e]
=C...C	2.425(2)	−0.0110	0.0576	0.0578	0.0016(14)[e]
C...O(n)	2.447(4)	−0.0074	0.0625	0.0626	0.0016(14)[e]
=C...O	3.482(3)	−0.0064	0.0564	0.0574	0.0060(30)[f]
C...O(f)	3.600(3)	−0.0097	0.0603	0.0607	0.0060(30)[f]
O...O	4.566(5)	0.0000	0.0623	0.0639	0.0086(47)

[a] In Å, $T = 392$ K. Root-mean-square amplitudes u were calculated using the traditional scheme (h0) and taking into account nonlinear kinematic effects at the level of the first-order perturbation theory (h1). Superscript fr corresponds to the frame structure (see text). The values in parentheses are the estimated total errors (3σ for r_e and 2σ for u). [b] Notation: O(n), nearest, and O(f), farthest oxygen atoms relative to the given carbon atom. [c] Assumed. [d] Experimental amplitudes were refined in one group with retaining the differences between the calculated amplitudes of this group. [e] See footnote d. [f] See footnote d.

the overall rotation ($\delta_{ij}^{\mathrm{cent,rot}}$[33]) were also included. The total corrections ($r_{ij,\mathrm{e}} - r_{ij,\mathrm{a}}$) and the rms vibrational amplitudes (u_{ij}) calculated by means of SHRINK-07 program are listed in Tables 3 and 6S (Supporting Information) for the dynamic and static molecular models, respectively. The fitting of the GED intensities was performed using the KCED25 program[34] adapted for personal computer at the Eötvös Budapest University (Hungary) and modified at the Moscow State University.

Static Model. The molecular structure was preliminarily studied using a so-called static model traditionally applied in the GED analysis. On the basis of the C_{2v} symmetry, it was described by 10 independent parameters: N−H, N−C, =C−C, C=O, and C−H bond lengths; CNH, NCC, NC=O, and =CCH bond angles; and HCCN dihedral angle. The refined values are listed in Table 4. As can be seen, the determined parameters of the nonrigid −CH$_2$−CH$_2$− fragment are different from those calculated at the MP2(full)/6−311G(3df,2p) level, whereas the parameters of the rigid part are in good agreement. The large differences between the rms vibrational amplitudes u_{h1} and those calculated in the traditional approximation u_{h0} (0.006 and 0.013 Å for the =C...C and C...O(f) terms, respectively) point also to the nonrigidity of the molecular fragment.[35] The radial distribution curve $f(r)$ shows also remarkable discrepancies between the experimental and theoretical curves in the ranges of the C−C, =C...C, C...O(n), and C...O(f) and other distances between the atoms involved in the large-amplitude ring-twisting motion (see Figure 4; for definition of the C...O(f) and C...O(n) distances, see footnote b to Table 3).

To adequately describe the molecular dynamics of the succinimide molecule, we applied in the following analysis the so-called dynamic model.

Dynamic Model. The potential function of the ring-twisting motion $V(\varphi)$ from the MP2(full)/6−311G(3df,2p) calculations with the Fourier coefficients V_0, V_3, and V_5, determined as shown above (see section 5) and as presented in Table 2, was used in the following GED analysis. The equilibrium conformation in the dynamic model was described by the same set of parameters as in the static model except for the =C−C distance and NCC

TABLE 4: Equilibrium Parameters of Succinimide Molecule (C_{2v} Symmetry) from GED Data and MP2(Full) Calculations[a]

	GED[b]		MP2(full)
parameter	dynamic model[c]	static model	6−311G(3df,2p)
N−H	1.007(18)	1.009[d]	1.0090
C−H	1.086(7)	1.091(12)	1.0871
C=O	1.202(1)	1.202(3)	1.2036
N−C	1.376(2)	1.382(3)	1.3840
=C−C	1.520(4)[e]	1.522(6)	1.5154
C−C	1.526(5)	1.553(15)[e]	1.5248
C−N−C	116.5(4)[e]	117.5(7)[e]	115.12
N−C−C	106.3(3)[e]	105.8(6)	106.92
C−C−C	105.5(2)[e]	105.4(3)[e]	105.53
C−N−H	121.8(2)	121.3(3)	122.44
N−C=O	126.1(4)	126.1(7)	125.23
C−C=O	127.6(2)[e]	128.1(3)[e]	127.86
=C−C−H	109.7(14)	115.1(23)	108.30
C−C−H	112.7(12)[e]	105.5(25)[e]	113.58
H−C−H	106.5(29)[e]	109.2(25)[e]	107.35
H−C−C−N	±121.7(14)	±115.9(30)	±121.94
H−N−C=O	0.00	0.00	0.00
R_f, %	2.77	4.56	

[a] Bond lengths in Å, bond angles and torsion angles in °. [b] The values in parentheses are 3 times the estimated standard errors (3σ). R_f is goodness of fit of the theoretical molecular intensities to the experimental ones. [c] Equilibrium independent parameter N...X, where X is the middle of C−C bond (see text), was determined to be 2.189(5) Å. [d] Assumed at the value from MP2(full)/6−311G(3df,2p) calculations. [e] Dependent parameter.

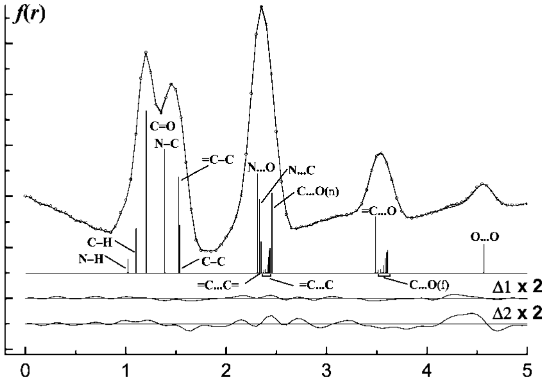

Figure 4. Experimental (points) with damping factor of exp(−0.002s^2) and theoretical (solid line) for the dynamic model radial distribution curves $f(r)$ and their difference curve Δ1 in comparison with the difference curve Δ2 for the static model.

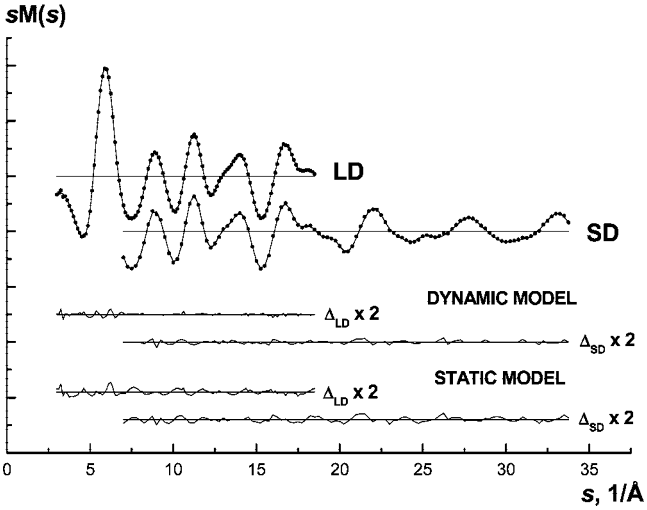

Figure 5. Experimental (points) and theoretical (for the final dynamic model, solid line) molecular intensity curves $sM(s)$ for the long (LD) and short (SD) nozzle-to-film distances and their difference curves Δ in comparison with those for the static model.

angle which were replaced by the C−C bond length and auxiliary N...X distance along the C_2 molecular axis, where X is the middle of the C−C bond. The ring-twisting motion was modeled by a set of six semirigid pseudoconformers of C_2 symmetry; each of these had a ring-twisting angle φ averaged over the corresponding subinterval of the coordinate φ ranging from 0° to 30°. The relative weights of each subinterval were determined with respect to the equilibrium value $\varphi = 0°$ according to the Boltzman distribution. The semirigid pseudoconformers were treated as distinct molecules undergoing the usual vibrations except for the ring-twisting motion around the C_2 molecular axis, that is, frame vibrations. The geometrical parameters of the equilibrium conformation ($\varphi = 0°$) were refined in the least-squares analysis, while the molecular parameters of the pseudoconformers were deduced by adding the relaxation differences to the refined values. The relaxation effects were derived from the MP2(full)/6−311G(3df,2p) calculations (see section 5). The harmonic and anharmonic corrections to the internuclear distances as well as the rms vibrational amplitudes (u_{h0}^{fr} and u_{h1}^{fr}) were calculated including the contributions from all normal modes except for the ring-twisting motion, which was found to be a pure mode (see section 4) and therefore which could be separated. As can be seen from Table 3, the agreement between the u_{h1}^{fr} and u_{h0}^{fr} values for the =C...C and C...O(f) terms is considerably better in comparison to that between u_{h1} and u_{h0} calculated for the static model. It confirms that the ring-twisting motion is the main contributor to the nonrigidity of the molecule. Being independent from the large-amplitude motion in the frame structure, the rms amplitudes for all distances of ca. 2.4 and 3.5 Å could be more effectively refined in groups than it was possible in the case of the static model.

The experimental molecular intensity $sM(s)$ and radial distribution $f(r)$ curves with their theoretical analogues for the final dynamic molecular model are shown in Figures 5 and 4, respectively.

Discussion and Conclusions

In the MP2(full) calculations with 6−311G(2df,p), cc-pVTZ, and 6−311G(3df,2p) basis sets (see section 3), the conformation of succinimide is found to have C_{2v} symmetry, whereas in the MP2(full)/6−311G(d,p) approximation, the molecule is predicted to be of C_2 symmetry. Yielding contradictory results concerning the conformation of the molecule, our calculations present an additional example of the appearance of two-electron basis set incompleteness errors (BSIEs) analyzed in several studies.[36] These errors may arise in arenes as well as in carbon compounds with multiply bonded moieties,[37−40] among others, in amides with the peptide fragment −(O=)C−N<.[41,42] To balance such errors, for example, the polarization f-function should be included.[36,37,41−44] The correlation-consistent (aug)-cc-pVTZ basis set[45] is fundamentally constructed to provide the necessary BSIE balance. Therefore, the cc-pVTZ and 6−311G (3df,2p) basis sets are good choices to determine the equilibrium conformation of succinimide by the MP2 method. The structural parameters calculated with these basis sets are very close to each other and to those from the GED data.

Since the flexibility of the five-membered ring system like succinimide has not been studied yet, it was necessary to create an appropriate model describing the dynamics of this molecule. The experimental vibrational spectra were reliably interpreted using a scaled force field from the MP2(full)/6−311G(3df,2p) calculations. The analysis of vibrational spectra has shown that the ring-twisting and ring-bending, which belong to different symmetry types, are practically pure modes. The cross sections of the potential energy surface along the ring-bending and ring-twisting coordinates in the MP2/6−311G(3df,2p) approximation were determined to be almost harmonic and strongly anharmonic functions, respectively.

As it was demonstrated for simple amides, such as $H_2NC(=O)H$, $Me_2NC(=O)H$, and $Me_2NC(=O)Cl$,[42,46] the internal rotation around the N−C(=O) bond with the high barrier to rotation of 15−20 kcal/mol would need an elongation of this bond in the transition state relative to the equilibrium position by up to 0.05−0.06 Å. Since the r_e(N−C(=O)) bond in succinimide is already by 0.02−0.03 Å longer than that in amides, it can be expected that the torsion motions around these bonds in succinimide are less hindered than in these amides. The reduction of hindrance led to an amplification of the ring-twisting vibrations and thus is a reason of the flexibility in the strain ring.

At the same time, the ring-bending motion in succinimide, which correlates with the pyramidal distortion of both rigid carbonyl fragments, requires a considerable energetic consumption. Therefore, this motion could not be a reason of the ring flexibility. The practically harmonic character of the potential function of this motion confirms this conclusion. For the ring-bending vibration, the frequency and quadratic force constant values (see section 4) are considerably larger in comparison to those for the ring-twisting vibration. Hence, just the ring-twisting motion is a principal reason for the flexibility of the succinimide ring.

Being independent, the large-amplitude anharmonic ring-twisting motion could be described separately from the remaining relatively small-amplitude vibrations of the molecule. The flexibility of succinimide because of the large-amplitude ring-twisting motion has been taken into account in the GED analysis applying the dynamic model which greatly improved the agreement between the experimental and theoretical reduced molecular scattering intensities, $sM(s)$, ($R_f = 2.8\%$) in comparison to that for the static GED model ($R_f = 4.6\%$) as shown in Figure 5. The differences between $\Delta f(r)$ curves for the dynamic and static models show the remarkable contribution of the flexibility effect to the experimental data (see Figure 4). The equilibrium molecular parameters involved in the ring-twisting motion (C−C, =C−C−H, C−C−H, and H−C−C−N) obtained in the dynamic approximation are very close to the corresponding values from the ab initio calculations (see Table 4), whereas they considerably deviate from those for the static model (C−C bond length by 0.027 Å, =C−C−H, C−C−H, and H−C−C−N angles by up to 7°). For the C−C bond length, the deviation due to flexibility influence is several times larger than the calculated vibrational correction ($r_e - r_a$) and the experimental uncertainty. It means that the large-amplitude ring-twisting motion has to be considered in the GED analysis of succinimide.

Acknowledgment. This research was supported by the Dr. Barbara Mez-Starck Foundation (Germany) and the Russian Foundation for Basic Research (Grant No. 08-03-00507).

Supporting Information Available: Experimental intensity curves with final backgrounds (Table 1S); equilibrium parameters of succinimide molecule from MP2(full) calculations with different basis sets (Table 2S); nonredundant set of the local symmetry internal coordinates and the scale factors for the MP2(full)/6−311G(3df,2p) force field (Table 3S); band assignment in the spectra of succinimide on the basis of the MP2(full)/6−311G(3df,2p) force field using the scaling procedure (Table 4S); force constants in internal coordinates for the succinimide molecule from the MP2(full)/6−311G(3df,2p) calculations after scaling (Table 5S); vibrational corrections to the experimental internuclear distances and rms vibrational amplitudes for the static molecular model (Table 6S); experimental intensity curves $I(s)$ with the background lines for the long and short nozzle-to-film distances (Figure 1S); potential curve of the ring-bending motion $V(x)$ from the MP2(full)/6−311G(3df,2p) calculations (Figure 2S); variations of the nonbonded interatomic distances as a function of the ring-twisting coordinate φ (Figure 3S); potential curve of the ring-twisting motion $V(\varphi)$ from the MP2(full)/6−311G(3df,2p) calculations (Figure 4S). This information is available free of charge via the Internet at http://pubs.acs.org.

References and Notes

(1) Adams, W. J.; Geise, H. J.; Bartell, L. S. *J. Am. Chem. Soc.* **1970**, *92*, 5013.

(2) Brendhaugen, K.; Kolderup-Fikke, M.; Seip, H. M. *Acta Chem. Scand.* **1993**, *27*, 1101.

(3) Blanco, S.; Lopez, J. C.; Lesarri, A.; Alonso, J. L. *J. Am. Chem. Soc.* **2006**, *128*, 12111.

(4) Legon, A. C. *Chem. Rev.* **1980**, *80*, 231.

(5) Laane, J. *Annu. Rev. Phys. Chem.* **1994**, *45*, 179.

(6) Laane, J. *Intern. Rev. Phys. Chem.* **1999**, *18*, 301.

(7) Laane, J. *J. Phys. Chem.* **2000**, *104*, 7715.

(8) Vogt, J.; Vogt, N. *J. Mol. Struct.* **2004**, *695*, 237.

(9) *Structure of Free Polyatomic Molecules, Landolt-Börnstein, New Series*; Kuchitsu, K., Vogt, N., Tanimoto, M., Eds.; Springer: Berlin, Germany, 2007; Vol. II/28C.

(10) *Structure of Free Polyatomic Molecules, Landolt-Börnstein, New Series*; Kuchitsu, K., Ed.; Springer: Berlin, Germany, 2000; Vol. II/25C.

(11) Katritzky, A. R.; Yao, J.; Qi, M.; Chou, Y.; Sikora, D. J.; Davis, S. *Hetorocycles* **1998**, *48*, 2677.

(12) Montalbetti, C. A. G. N.; Falque, V. *Tetrahedron* **2005**, *61*, 10827.

(13) Vogt, N.; Khaikin, L.; Grikina, O. E.; Rykov, A. N.; Vogt, J. *J. Phys. Chem. A* **2008**, *112*, 7662.

(14) Shibata, S.; Jejeina, K.; Tani, R.; Nakanuita, J. *Rep. Fac. Sci. Pleizieoka Univ.* **1974**, 9.

(15) Vishnevskiy, Y. V. *J. Mol. Struct.* **2007**, *833*, 30.

(16) Frisch, M. J.; Trucks, G. W.; Schlegel, H. B.; Scuseria, G. E.; Robb, M. A.; Cheeseman, J. R.; Montgomery, J. A., Jr.; Vreven, T.; Kudin, K. N.; Burant, J. C.; Millam, J. M.; Iyengar, S. S.; Tomasi, J.; Barone, V.; Mennucci, B.; Cossi, M.; Scalmani, G.; Rega, N.; Petersson, G. A.; Nakatsuji, H.; Hada, M.; Ehara, M.; Toyota, K.; Fukuda, R.; Hasegawa, J.; Ishida, M.; Nakajima, T.; Honda, Y.; Kitao, O.; Nakai, H.; Klene, M.; Li, X.; Knox, J. E.; Hratchian, H. P.; Cross, J. B.; Adamo, C.; Jaramillo, J.; Gomperts, R.; Stratmann, R. E.; Yazyev, O.; Austin, A. J.; Cammi, R.; Pomelli, C.; Ochterski, J. W.; Ayala, P. Y.; Morokuma, K.; Voth, G. A.; Salvador, P.; Dannenberg, J. J.; Zakrzewski, V. G.; Dapprich, S.; Daniels, A. D.; Strain, M. C.; Farkas, O.; Malick, D. K.; Rabuck, A. D.; Raghavachari, K.; Foresman, J. B.; Ortiz, J. V.; Cui, Q.; Baboul, A. G.; Clifford, S.; Cioslowski, J.; Stefanov, B. B.; Liu, G.; Liashenko, A.; Piskorz, P.; Komaromi, I.; Martin, R. L.; Fox, D. J.; Keith, T.; Al-Laham, M. A.; Peng, C. Y.; Nanayakkara, A.; Challacombe, M.; Gill, P. M. W.; Johnson, B.; Chen, W.; Wong, M. W.; Gonzalez, C.; Pople, J. A. *Gaussian 03* , revision B.03; Gaussian, Inc.: Pittsburgh PA, 2003.

(17) Woldbæk, T.; Klæboe, P.; Christensen, D. H. *Acta Chem. Scand. A* **1976**, *30*, 531.

(18) Stamboliyska, B. A.; Binev, Y. I.; Radomirska, V. B.; Tsenov, J. A.; Juchnovski, I. N. *J. Mol. Struct.* **2000**, *516*, 237.

(19) Parellada, R.; Gomez, V.; Arenas, J. *An. Quim.* **1974**, *70*, 753.

(20) Uno, T.; Machida, K. *Bull. Chem. Soc. Jpn.* **1962**, *35*, 276.

(21) Fogarasi, G.; Pulay, P. *Vib. Spectra Struct.* **1985**, *14*, 125.

(22) Pulay, P.; Fogarashi, G.; Pongor, G.; Boggs, J. E.; Vargha, A. *J. Am. Chem. Soc.* **1983**, *105*, 7037.

(23) Krasnoshchekov, S. V.; Abramenkov, A. V.; Panchenko, Y. N. *Zh. Fiz. Khim.* **1997**, *71*, 497.

(24) Csaszar, P.; Csaszar, A.; Harsanyi, L.; Boggs, J. E. *J. Mol. Struct.* **1986**, *136*, 323–337.

(25) Sipachev, V. A. *J. Mol. Struct. (THEOCHEM)* **1985**, *121*, 143.

(26) Sipachev, V. A. *Advances in Molecular Structure Research* **1999**, *5*, 263.

(27) Ueda, T.; Shimanouchi, T. *J. Chem. Phys.* **1967**, *47*, 4042.

(28) Laane, J.; Harthcock, M. A.; Killough, P. M.; Bauman, L. E.; Cooke, J. M. *J. Mol. Spectrosc.* **1982**, *91*, 286.

(29) Harthcock, M. A.; Laane, J. *J. Mol. Spectrosc.* **1982**, *91*, 300.

(30) Abramenkov, A. V. *Zh. Fiz. Khim.* **1995**, *69*, 1048.

(31) Sipachev, V. A. *Struct. Chem.* **2000**, *11*, 167.

(32) Sipachev, V. A. *J. Mol. Struct.* **2001**, *567−568*, 67.

(33) Iwasaki, M.; Hedberg, K. *J. Chem. Phys.* **1962**, *36*, 2961.

(34) Gundersen, G.; Samdal, S.; Seip, H. M. *Least Squares Structural Refinement Program Based on Gas Electron Diffraction Data*; University of Oslo: Oslo, Norway, 1981.

(35) Khaikin, L. S.; Grikina, O. E.; Granovsky, A. A.; Nikitin, V. S.; Vilkov, L. V. *Struct. Chem.* **2004**, *15* (1), 17.

(36) Moran, D.; Simmonett, A. C.; Leach, F. E.; Allen, W. D.; Shleyer, P. v. R.; Schaefer, H. F. *J. Am. Chem. Soc.* **2006**, *128*, 9342.

(37) Simandiras, E. D.; Rice, J. E.; Lee, T. J.; Amos, R. D.; Handy, N. C. *J. Chem. Phys.* **1988**, *88*, 3187.

(38) Lee, T. J.; Allen, W. D.; Schaefer, H. F. *J. Chem. Phys.* **1987**, *87*, 7062.

(39) Breidung, J.; Schneider, W.; Thiel, W.; Lee, T. J. *J. Chem. Phys.* **1992**, *97*, 3498.

(40) Martin, J. M. L.; Lee, T. J.; Taylor, P. R. *J. Chem. Phys.* **1998**, *108*, 676.

(41) Fogarasi, G.; Szalay, P. G. *J. Phys. Chem. A* **1997**, *101*, 1400.

(42) Khaikin, L. S.; Grikina, O. E.; Abramenkov, A. V.; Stepanov, N. F. *Zh. Fiz. Khim.* **2005**, *79*, 693.

(43) Khaikin, L. S.; Grikina, O. E.; Stepanov, N. F. *Zh. Fiz. Khim.* **2005**, *79*, 861.

(44) Khaikin, L. S.; Grikina, O. E.; Stepanov, N. F.; Kovacs, A. *Zh. Fiz. Khim.* **2005**, *79*, 1101.

(45) Dunning, T. H. *J. Chem. Phys.* **1989**, *90*, 1007.

(46) Khaikin, L. S.; Grikina, O. E.; Kovacs, A.; Vilkov, L. V. *Zh. Fiz. Khim.* **2005**, *79*, 1269.

JP8089177